

# Anharmonic calculations of the optical-phonon lifetime for crystals with the diamond structure

E. Haro-Poniatowski and J. L. Escamilla-Reyes

*Departamento de Física, Laboratorio de Optica Cuántica, Universidad Autonoma Metropolitana Iztapalapa, Apartado Postal 55-534, México 09340, Distrito Federal, Mexico*

K. H. Wanser

*Department of Physics, California State University Fullerton, Fullerton, California 92634-9480*

(Received 8 June 1995)

Anharmonic calculations of crystals having the diamond structure; silicon, germanium, diamond, and alpha-tin are reported. The principal channels of decay of the optical phonon are determined for each material. In particular the zone-center phonon lifetime is computed with the exception of alpha-tin. A reasonable agreement between theory and experiment is obtained considering the simplicity of the harmonic and anharmonic models employed in the present calculation. The linewidth of the optical phonon at a temperature of 10 K is found to be  $1.19 \text{ cm}^{-1}$  for silicon,  $0.53 \text{ cm}^{-1}$  for germanium, and  $0.84 \text{ cm}^{-1}$  for diamond the experimental values being 1.24, 0.75, and  $1.68 \text{ cm}^{-1}$ , respectively. [S0163-1829(96)06718-5]

## I. INTRODUCTION

Anharmonic processes have been studied extensively by inelastic light scattering in crystals with the diamond structure.<sup>1-4</sup> Very recently results have been reported on the anharmonic effects in silicon and germanium alloys and heterostructures.<sup>5,6</sup> Raman analysis has been performed over a wide range of temperatures in the cases of silicon and germanium. The effect of temperature is to decrease the Raman shift and to increase the linewidth of the optical phonon. The temperature dependence of the optical mode has been used to probe the temperature profile of conventionally heated and laser-heated silicon.

Theoretically several types of models have been used to describe the temperature dependence of the Raman mode. These models have been applied in most of the cases to silicon. In particular, Cowley<sup>7,8</sup> has investigated the cases of silicon, diamond, and germanium. An essential ingredient for the theoretical models developed are the Fourier-transformed anharmonic coefficients that enter into the expressions of the damping constant and the frequency shift of the optical phonon.<sup>9</sup> However these computations are rather complex and were in the past frequently simplified by approximating the anharmonic coefficients by simpler expressions.<sup>1</sup> For a long time the principal theoretical calculation was that of Cowley.<sup>7,8</sup> This calculation was later improved by Haro *et al.*<sup>9</sup> A few years ago a realistic *ab initio* calculation of the contribution to the inverse lifetime and frequency shift of phonons in silicon was performed by Narasimhan and Vanderbilt.<sup>10</sup> At the same time a molecular-dynamics study of anharmonic effects in silicon was done by Wang, Chan, and Ho.<sup>11</sup> Both calculations give good agreement with experiment. Recently Koval and Migoni<sup>12</sup> did a consistent anharmonic shell-model calculation for the Raman mode in silicon. These authors claim that polarizability effects are essential to give a good description of the experimental results. In the present work we give a description of the anharmonic properties of C, Si, Ge, and  $\alpha$ -Sn using simple harmonic and anharmonic models.<sup>9,13</sup> The possible channels of

decay are identified for each material. Furthermore the corresponding linewidths are computed for Si, Ge, and C. Due to the lack of experimental data regarding the third-order elastic constants we were unable to compute these quantities for  $\alpha$ -Sn. Considering the simplicity of the models used our calculations compare quite reasonably with the experimental results.

### A. Anharmonicity in crystals; central potentials

Let us restrict our analysis to central potentials and only consider the cubic term in the vibrational Hamiltonian:<sup>14,15</sup>

$$\Phi_{3c} = \frac{1}{12} \sum_{l,\kappa} \sum_{l',\kappa'} \sum_{\alpha\beta\gamma} \phi_{\alpha\beta\gamma}(l\kappa|l'\kappa') u_{\alpha}(l\kappa|l'\kappa') \times u_{\beta}(l\kappa|l'\kappa') u_{\gamma}(l\kappa|l'\kappa'), \quad (1.1)$$

where

$$\begin{aligned} \phi_{\alpha\beta\gamma}(l\kappa|l'\kappa') = & \left\{ \frac{x_{\alpha}x_{\beta}x_{\gamma}}{r^3} \left[ \phi_{\kappa\kappa'}'''(r) - \frac{3}{r} \phi_{\kappa\kappa'}''(r) \right. \right. \\ & \left. \left. + \frac{3}{r^2} \phi_{\kappa\kappa'}'(r) \right] + \frac{(x_{\alpha}\delta_{\beta\gamma} + x_{\beta}\delta_{\alpha\gamma} + x_{\gamma}\delta_{\alpha\beta})}{r^2} \right. \\ & \left. \times \left[ \phi_{\kappa\kappa'}''(r) - \frac{1}{r} \phi_{\kappa\kappa'}'(r) \right] \right\}_{\mathbf{r}=\mathbf{R}(l\kappa|l'\kappa')} \quad (1.2) \end{aligned}$$

with

$$\mathbf{r} = \sum_{\alpha} x_{\alpha} \hat{e}_{\alpha} \quad \text{and} \quad \mathbf{R}(l\kappa|l'\kappa') = \mathbf{R}(l\kappa) - \mathbf{R}(l'\kappa') \quad (1.3)$$

and

$$\phi'(r) = \frac{d\phi(r)}{dr}, \quad \phi''(r) = \frac{d^2\phi(r)}{dr^2}, \quad \phi'''(r) = \frac{d^3\phi(r)}{dr^3}. \quad (1.4)$$

TABLE I. Values of the parameters used in the harmonic model described in the text.

	$\omega_{\text{RA}}$ ( $\text{s}^{-1}$ )	$\omega_{\text{TAX}}$ ( $\text{s}^{-1}$ )	$b$ dyn/(cm esu <sup>2</sup> )	$\alpha$ (dyn/cm)	$\mu$ (dyn/cm)	$\sigma$ (dyn/cm)	$p_1^2$ (esu)
C	$2.51 \times 10^{14}$	$1.52 \times 10^{14}$	$-3.39 \times 10^{22}$	$4.44 \times 10^4$	$2.12 \times 10^4$	$4.23 \times 10^4$	$6.87 \times 10^{-20}$
Si	$9.8 \times 10^{13}$	$2.8 \times 10^{13}$	$-2.28 \times 10^{22}$	$3.67 \times 10^4$	$3.077 \times 10^3$	$7.179 \times 10^3$	$3.05 \times 10^{-20}$
Ge	$5.73 \times 10^{13}$	$1.50 \times 10^{13}$	$-2.53 \times 10^{23}$	$3.26 \times 10^4$	$1.86 \times 10^3$	$6.36 \times 10^3$	$2.23 \times 10^{-19}$
Sn	$3.77 \times 10^{13}$	$7.54 \times 10^{12}$	$-9.93 \times 10^{21}$	$5.706 \times 10^4$	$5.706 \times 10^2$	$3.914 \times 10^3$	$3.23 \times 10^{-19}$

We are interested in this work in the particular case of the disintegration of the optical phonon at the zone center (Raman mode), into two phonons (cubic process). The zone-center phonon has a zero wave vector; the conservation laws of momentum and energy give in this case

$$\omega(\mathbf{q}', j') + \omega(\mathbf{q}'', j'') = \omega(\mathbf{0}, j),$$

$$\mathbf{q}' + \mathbf{q}'' = \mathbf{0} \Rightarrow \mathbf{q}'' = -\mathbf{q}', \quad (1.5)$$

the corresponding Fourier-transformed anharmonic coefficients are given by<sup>9</sup>

$$V(\mathbf{0}, j; \mathbf{q}, j'; -\mathbf{q}, j'') = \frac{N}{12} \left[ \frac{\hbar}{2NM} \right]^{3/2} (\omega_{\mathbf{0}, j} \omega_{\mathbf{q}, j'} \omega_{-\mathbf{q}, j''})^{-1/2} \sum_{\alpha\beta\gamma} \sum_{l'\kappa\kappa'} \Phi_{\alpha\beta\gamma}(0, \kappa | l', \kappa') [e_{\alpha}(\kappa | \mathbf{0}, j) - e_{\alpha}(\kappa' | \mathbf{0}, j)] \\ \times [e_{\beta}(\kappa | \mathbf{q}, j') - e_{\beta}(\kappa' | \mathbf{q}, j')] e^{i[\mathbf{q} \cdot \mathbf{R}(l')]} [e_{\gamma}(\kappa | -\mathbf{q}, j'') - e_{\gamma}(\kappa' | -\mathbf{q}, j'')] e^{-i[\mathbf{q} \cdot \mathbf{R}(l')]} \quad (1.6)$$

the linewidth and frequency shift of the zone-center optical phonon are given by

$$\Gamma(\mathbf{0}, j, \omega) = \frac{18}{\hbar^2} \sum_{\mathbf{q}} \sum_{j_1 j_2} |V(\mathbf{0}, j; \mathbf{q}, j_1; -\mathbf{q}, j_2)|^2 \{ (n_1 + n_2 + 1) [\delta(\omega - \omega_1 - \omega_2) - \delta(\omega + \omega_1 + \omega_2)] \\ + (n_1 - n_2) [\delta(\omega + \omega_1 - \omega_2) - \delta(\omega - \omega_1 + \omega_2)] \}, \quad (1.7)$$

$$\Delta(\mathbf{0}, j, \omega) = -\frac{18}{\hbar^2} \sum_{\mathbf{q}} \sum_{j_1 j_2} |V(\mathbf{0}, j; \mathbf{q}, j_1; -\mathbf{q}, j_2)|^2 P \left\{ \frac{n_1 + n_2 + 1}{\omega + \omega_1 + \omega_2} - \frac{n_1 + n_2 + 1}{\omega - \omega_1 - \omega_2} + \frac{n_1 - n_2}{\omega + \omega_1 - \omega_2} - \frac{n_1 - n_2}{\omega - \omega_1 + \omega_2} \right\}. \quad (1.8)$$

These two expressions are related by the Kramers-Kronig transformation.

## II. HARMONIC MODEL

In order to compute the eigenfrequencies and eigenvectors appearing in the previous expressions one needs to use a harmonic model. Wanser and Wallis have studied thermal expansion of silicon using a harmonic model which includes first- through fourth-neighbor central interactions, angle bending interactions, and nonlocal dipole interactions. These interactions can be characterized by 11 parameters.<sup>9,13,16</sup> These authors have developed a simpler version of the model

with only four parameters which can be determined from experimental values. This simpler model gives a satisfactory description of the acoustical branches of the phonon-dispersion curves. As it will be shown later the principal channels of decay of the Raman mode involve acoustical branches.

The parameters are  $\alpha$ ,  $\mu$ ,  $\sigma$  and  $p_1 = z_1 e$ . These correspond to purely central forces, first- ( $\alpha = \beta$ ) and second- ( $\mu = \nu$ ) neighbor interactions, angle bending ( $\sigma$ ), and diagonal nonlocal dipoles ( $p_1; p_2 = 0$ ).<sup>9,16</sup> The parameters are related to the Raman frequency and the second-order elastic constants by

TABLE II. Experimental values for second- and third-order elastic constants  $\Phi_1'''(r_1)$  is computed using Eq. (3.1).

	$a$ (Å)	$C_{11}$ (dyn/cm <sup>2</sup> )	$C_{12}$ (dyn/cm <sup>2</sup> )	$C_{111}$ (dyn/cm <sup>2</sup> )	$C_{112}$ (dyn/cm <sup>2</sup> )	$C_{123}$ (dyn/cm <sup>2</sup> )	$\Phi_1'''(r_1)$ (dyn/cm <sup>2</sup> )
C	$3.56 \times 10^{-8}$	$10.76 \times 10^{12}$	$1.25 \times 10^{12}$	$-62.6 \times 10^{12}$	$-22.6 \times 10^{12}$	$1.12 \times 10^{12}$	$-36.0 \times 10^{13}$
Si	$5.4 \times 10^{-8}$	$1.66 \times 10^{12}$	$0.64 \times 10^{12}$	$-8.25 \times 10^{12}$	$-4.51 \times 10^{12}$	$-0.64 \times 10^{12}$	$-6.41 \times 10^{13}$
Ge	$5.65 \times 10^{-8}$	$1.29 \times 10^{12}$	$0.48 \times 10^{12}$	$-8.1 \times 10^{12}$	$-5.0 \times 10^{12}$	$-2.36 \times 10^{12}$	$-5.55 \times 10^{13}$
Sn	$6.49 \times 10^{-8}$	$0.690 \times 10^{12}$	$0.293 \times 10^{12}$				

$$8\alpha + \frac{64}{3}\sigma = M\omega_{\text{RA}}^2,$$

$$8\mu + 12\sigma + 4\pi b p_1^2 = M\omega_{\text{TAX}}^2,$$

$$\alpha + 4\mu - 2\sigma = aC_{12},$$

$$\alpha + 8\mu + 4\sigma = aC_{11},$$

where  $a$  is the conventional cube edge and  $b$  is a constant as described in Ref. 16. The values of the parameters can be determined using the experimental values of the second-order elastic constants and the frequencies<sup>17</sup> and are given in Tables I and II.

### III. ANHARMONIC MODEL

One important advantage of the harmonic model employed previously is that it can be extended in a straightfor-

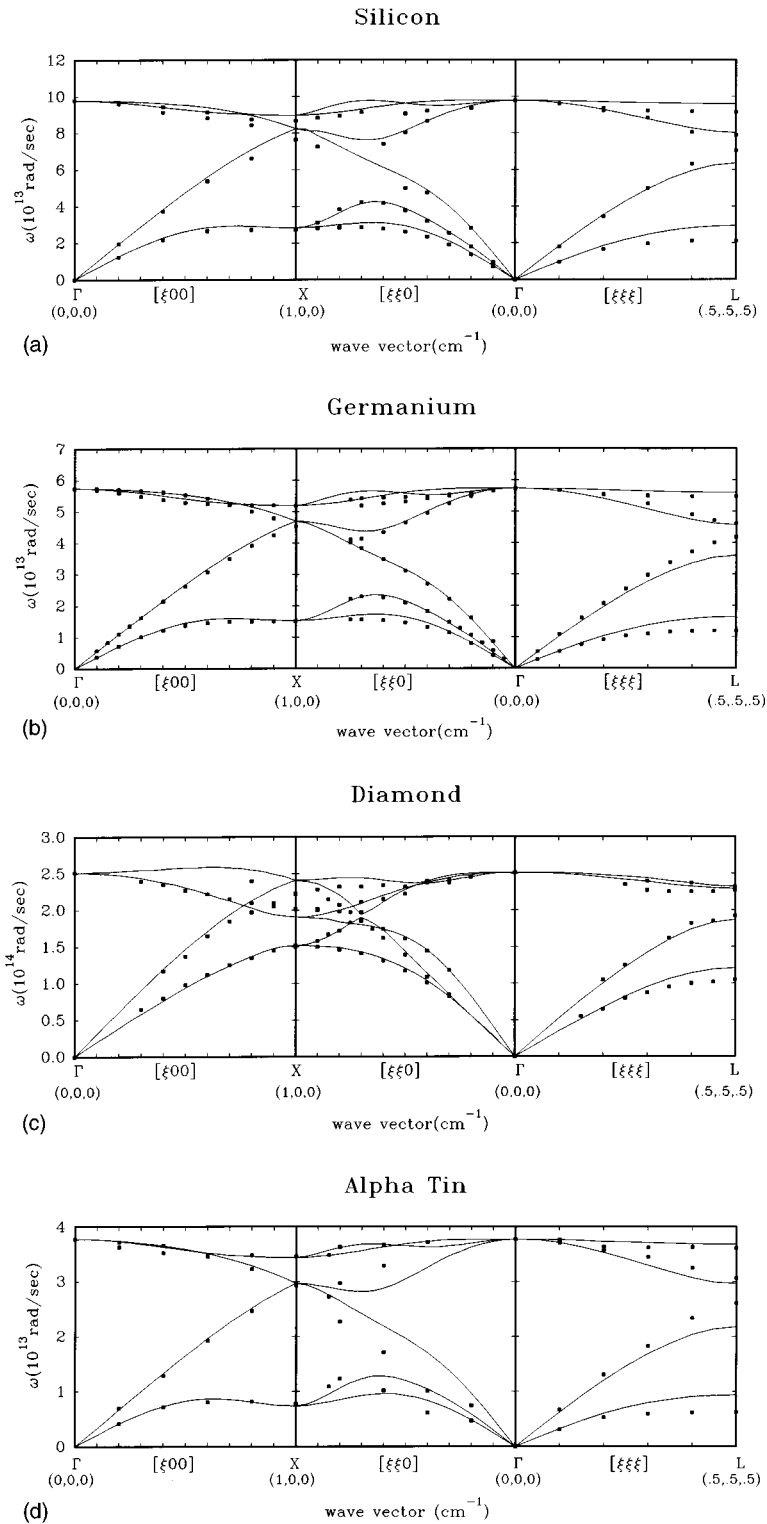


FIG. 1. Phonon-dispersion curves for (a) silicon, (b) germanium, (c) diamond, (d) alpha-tin using the harmonic model described in the text.

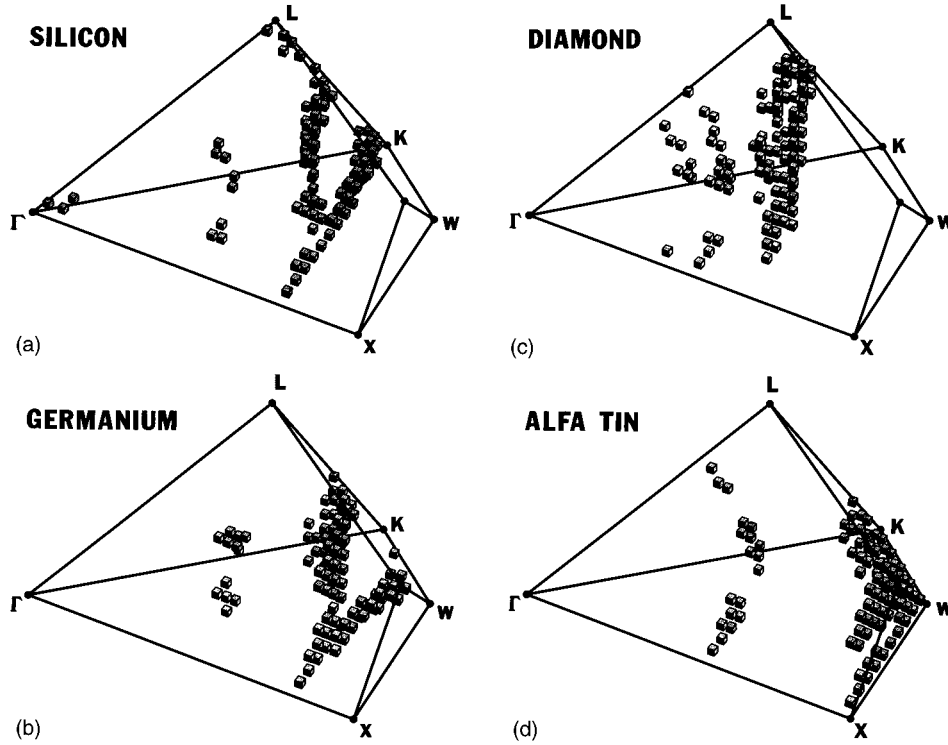


FIG. 2. 1/48th irreducible sector of the first Brillouin zone for (a) silicon, (b) germanium, (c) diamond, (d) alpha-tin. The cubes represent the possible channels of decay of the optical phonon.

ward fashion to include cubic anharmonic terms.<sup>9</sup> We restrict our attention to nearest-neighbor central interactions. With nearest-neighbor central interactions we have only one parameter to determine namely  $\phi_1'''(r_1)$  (where  $r_1$  is the first nearest-neighbor distance) given by<sup>9</sup>

$$\phi_1'''(r_1) = \left( \frac{4}{\sqrt{3}} \right) [C_{111} + 6C_{112} + 2C_{123} + 3C_{11} + 6C_{12}]. \quad (3.1)$$

The second- and third-order elastic constants for Si, Ge, and C have been measured,<sup>17</sup> these are given in Table II in this table are also given the corresponding values of  $\phi_1'''(r_1)$ . The first and second derivatives of the potential are given by  $\phi_1'(r_1) = 0$  and  $\phi_1''(r_1) = 3\alpha$ , respectively.<sup>16</sup> Note that in the case of  $\alpha$ -Sn only the second-order elastic constants have been measured.

TABLE III. Combinations of branches involved in the possible channels of decay for the optical phonon. The corresponding percentage of  $q$  points is given.

$j_1$	$j_2$	Silicon	Germanium	Diamond	Alpha-tin
1	1			40.5	
1	2			19.8	
1	3	47.1	28	10.8	
1	4	2.9			66.7
2	2			14.4	
2	3	42.3	59	7.2	
2	4				12.5
3	3	7.7	13	7.2	19.8

## IV. NUMERICAL CALCULATIONS

### A. Phonon-dispersion curves

Using the harmonic model described previously we have computed the phonon-dispersion relations for Si, Ge, C, and  $\alpha$ -Sn. The results are shown in Figs. 1(a)–1(d). The solid lines correspond to the present calculations and the plain circles are the experimental results.<sup>18–21</sup> In general the agreement is correct with the exception of the [111] direction where some difference occurs.<sup>16</sup>

### B. Channels of decay

In order to study the possible channels of decay of the zone-center optical phonon we have selected the  $\mathbf{q}$  points for which the frequency sum of any two phonon branches gives the Raman frequency

$$\omega_{j_1} + \omega_{j_2} = \omega_{\text{RA}} \pm 1\% \omega_{\text{RA}} \quad (4.1)$$

for  $J_1=1,6$  and  $J_2=16$ . This was done by generating a cubic mesh of 770 points inside the 1/48th sector of the Brillouin zone. The  $\mathbf{q}$  points satisfying relation (4.1) will represent the possible channels of decay for the zone-center optic mode. The fact of choosing 1% of the Raman frequency is closely related to the width of the Gaussian used to represent the  $\delta$  function appearing in expression (1.7). The width of this Gaussian is practically 1% of the Raman frequency. In actual practice this width must have a finite value that is sufficiently large to give a reasonable number of  $\mathbf{q}$  points a nontrivial weight and yet sufficiently small that the function is sharply peaked. When these conditions are fulfilled, the calculated

damping constant is sensibly independent of the width of the Gaussian.<sup>9</sup> In Figs. 2(a)–2(d) we show the selected  $\mathbf{q}$  points in the 1/48th irreducible sector of the Brillouin zone for C, Si, Ge, and  $\alpha$ -Sn. One observes marked differences between them. In particular the only case where one finds  $\mathbf{q}$  points near the  $\Gamma$  point is silicon. These points involve optical and acoustical combinations as possible channels of decay. In the cases of Si and Ge the pattern of points though similar is shifted one respect to the other. There is also a difference regarding the number of  $\mathbf{q}$  points satisfying relation (4.1) depending on the material. These numbers are 111, 98, 100, and 96 for C, Si, Ge, and  $\alpha$ -Sn, respectively. Using the same notation as Narasimhan and Vanderbilt<sup>10</sup> we have listed the different combination branches that represent possible chan-

nels of decay for the four materials studied in Table III. The branches are numbered in order of increasing energy; (1,2,3) correspond to acoustical branches and (4,5,6) to optical branches. For silicon the great majority of the possible channels involve pairs of acoustical branches, however one finds a small contribution of acoustical-optical pairs. In contrast to the results obtained in Ref. 10 no contribution of the type (2,2) were found in the present case. For germanium the situation is similar than for silicon. In the case of diamond all the possible acoustical combinations are present. Finally for alpha-tin one finds an important contribution of acoustical-optical branches. This can be explained by the significant depletion of the acoustical branches near the  $X$  point as seen in Fig. 1(d).

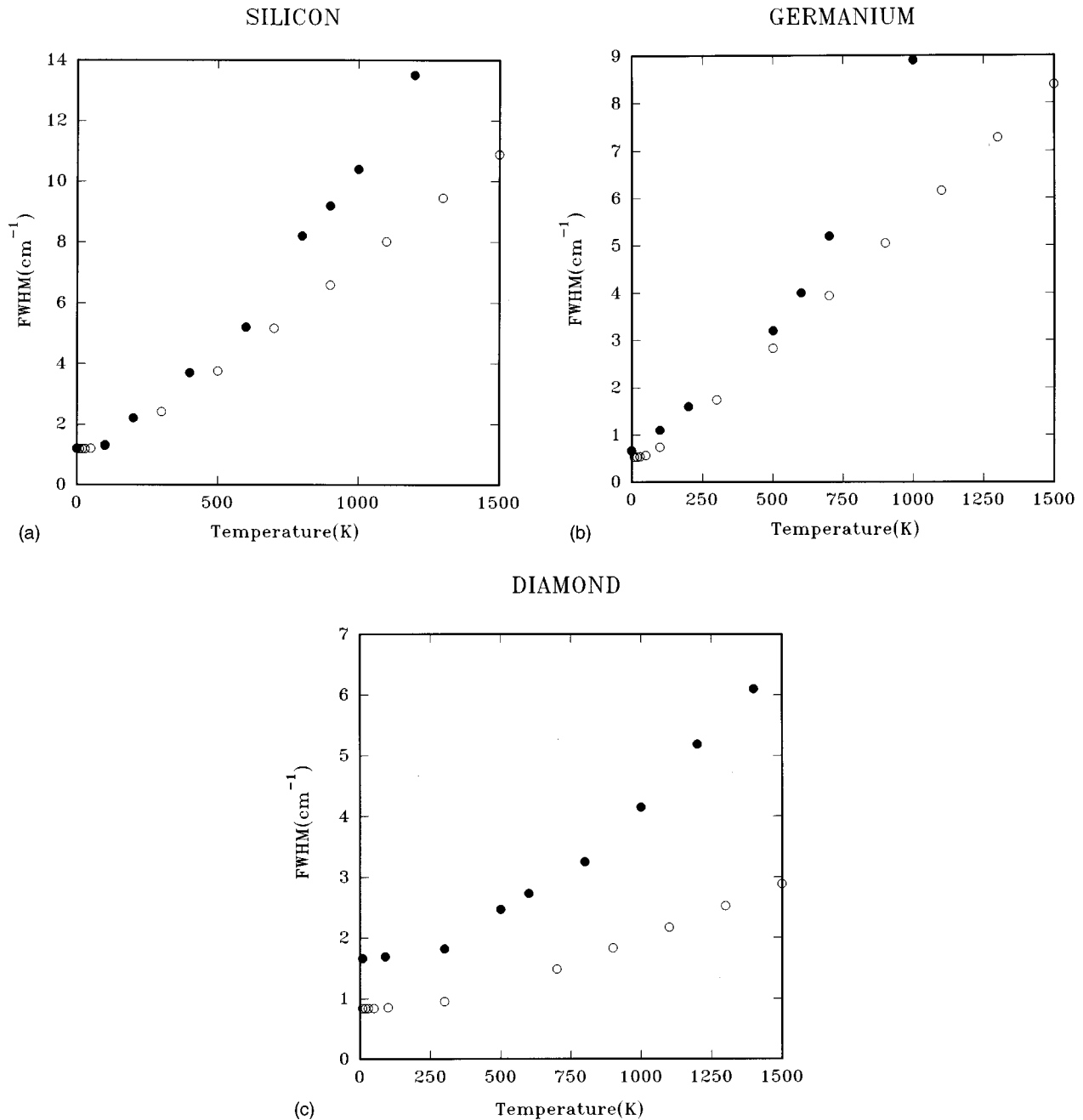


FIG. 3. Full widths at half maximum for (a) silicon, (b) germanium, (c) diamond. The full circles represent experimental values and the open circles the present calculations.

### C. Linewidth of the optical phonon

With the anharmonic model presented before, the Fourier-transformed anharmonic coefficients were computed. The sum over wave vectors was evaluated using the 770  $\mathbf{q}$  points cubic mesh as described in detail in Ref. 9. In Figs. 3(a)–3(c) the linewidth of the optical phonon is shown for the cases of silicon germanium and diamond. At low temperatures the agreement between theory and experiment is reasonable. For silicon and germanium the full width at half maximum (FWHM) are 1.19 and 0.53  $\text{cm}^{-1}$ , the corresponding experimental values<sup>3</sup> are 1.24 and 0.75  $\text{cm}^{-1}$ , respectively. As already discussed by other authors<sup>3,22</sup> the need to include higher-order anharmonic terms is evident above temperatures of the order of 500 K. In particular it has been shown that quartic terms have a significative contribution to the linewidth however they seem to have a less significative effect on the Raman shift.<sup>22</sup> For the case of diamond we have found a FWHM of 0.84  $\text{cm}^{-1}$  at 10 K as compared to 1.68  $\text{cm}^{-1}$  given by the experiment.<sup>23</sup>

### V. CONCLUSIONS

In this work we have determined the different channels of decay of the Raman mode for silicon, germanium, diamond, and alpha-tin. The corresponding linewidths were computed for silicon, germanium, and diamond. Considering the simplicity of the harmonic and anharmonic models employed in the present calculation the agreement between theory and experiment is good. Very recently Debernardi, Baroni, and Molinari have performed a first-principles calculation of anharmonic decay of phonons in diamond structure crystals, the agreement between theoretical results and experimental data is excellent.<sup>24</sup>

### ACKNOWLEDGMENTS

We gratefully acknowledge R. F. Wallis for his suggestions on the manuscript and M. Fernández-Guasti for his technical assistance. E.H.P. and J.L.E.R. acknowledge the financial assistance of CONACYT México.

- 
- <sup>1</sup>T. R. Hart, R. L. Aggarwal, and B. Lax, *Phys. Rev. B* **1**, 638 (1970).  
<sup>2</sup>M. Balkanski, R. F. Wallis, and E. Haro, *Phys. Rev. B* **28**, 1928 (1983).  
<sup>3</sup>J. Menéndez and M. Cardona, *Phys. Rev. B* **29**, 2051 (1984).  
<sup>4</sup>R. Tsu and J. Gonzalez Hernandez, *Appl. Phys. Lett.* **41**, 1016 (1982).  
<sup>5</sup>Hubert H. Buerke and Irving P. Herman, *Phys. Rev. B* **48**, 15 016 (1993).  
<sup>6</sup>Zhifeng Sui and Irving P. Herman, *Phys. Rev. B* **48**, 17 938 (1993).  
<sup>7</sup>R. A. Cowley, *Adv. Phys.* **12**, 421 (1963).  
<sup>8</sup>R. A. Cowley, *J. Phys. (Paris)* **26**, 659 (1965).  
<sup>9</sup>E. Haro, M. Balkanski, R. F. Wallis, and K. H. Wanser, *Phys. Rev. B* **34**, 5358 (1986).  
<sup>10</sup>Shobhana Narasimhan and David Vanderbilt, *Phys. Rev. B* **43**, 4541 (1991).  
<sup>11</sup>C. Z. Wang, C. T. Chan, and K. M. Ho, *Phys. Rev. B* **40**, 3390 (1989).  
<sup>12</sup>S. Koval and R. Migoni, *Phys. Rev. B* **49**, 998 (1994).  
<sup>13</sup>K. H. Wanser and R. F. Wallis, *J. Phys. (Paris) Colloq.* **42**, C6-128 (1981).  
<sup>14</sup>R. F. Wallis, I. P. Ipatova, and A. A. Maradudin, *Fiz. Tverd Tela (Leningrad)* **8**, 1064 (1966) [*Sov. Phys. Solid State* **8**, 850 (1966)].  
<sup>15</sup>I. P. Ipatova, A. A. Maradudin, and R. F. Wallis, *Phys. Rev.* **155**, 882 (1967).  
<sup>16</sup>K. H. Wanser, Ph.D. thesis, University of California, Irvine, 1982.  
<sup>17</sup>D. Bimberg, R. Blachnik, M. Cardona, P. J. Dean, Th. Grave, G. Harbeke, K. Hübner, U. Kaufmann, W. Kress, O. Madelung, W. von Münch, U. Rössler, J. Schneider, M. Schulz, and M. S. Skolnik, in *Numerical Data and Functional Relationships in Science and Technology*, edited by O. Madelung, M. Schulz, and H. Weiss, Landolt-Börnstein, New Series, Group III, Vol. 17 (Springer-Verlag, Heidelberg, 1982).  
<sup>18</sup>J. L. Warren, J. L. Yarnell, G. Dolling, and R. A. Cowley, *Phys. Rev.* **158**, 805 (1967).  
<sup>19</sup>G. Nilsson and G. Nelin, *Phys. Rev. B* **6**, 3777 (1972).  
<sup>20</sup>G. Nilsson and G. Nelin, *Phys. Rev. B* **3**, 364 (1971).  
<sup>21</sup>D. L. Price and J. M. Rowe, *Solid State Commun.* **7**, 1433 (1969).  
<sup>22</sup>H. Tang and I. P. Herman, *Phys. Rev. B* **43**, 2299 (1991).  
<sup>23</sup>W. J. Borer, S. S. Mitra, and K. V. Namjoshi, *Solid State Commun.* **9**, 1377 (1971).  
<sup>24</sup>A. Debernardi, S. Baroni, and E. Molinari, *Phys. Rev. Lett.* **75**, 1819 (1995).